(25) Zugenmaier, P. *J. Appl. Polym. Sci., Appl. Polym. Symp.* **1983**, *37*, 223.
(26) Zugenmaier, P.; Kuppel, A. *Colloid Polym. Sci.* **1986**, *264*, 231.
(27) De Santis, P.; Giglio, E.; Liquori, A. M.; Ripamonti, A. *J. Polym. Sci., Polym. Chem. Ed.* **1963**, 1383.
(28) De Santis, P.; Giglio, E.; Liquori, A. M.; Ripamonti, A. *Nature* **1965**, *206*, 456.
(29) Liquori, A. M.; De Santis, P.; Kovacs, A.; Mazzarella, L. *Nature* **1966**, *211*, 1039.
(30) Brant, D. A.; Flory, P. J. *J. Am. Chem. Soc.* **1965**, *87*, 2792.
(31) Brant, D. A.; Miller, W. G.; Flory, P. J. *J. Mol. Biol.* **1967**, *23*, 47.
(32) Tonelli, A. E.; Flory, P. J. *Macromolecules* **1969**, *2*, 225.
(33) Brant, D. A.; Tonelli, A. E.; Flory, P. J. *Macromolecules* **1969**, *2*, 228.
(34) Curl, R. F. *J. Chem. Phys.* **1959**, *30*, 1529.
(35) O'Gorman, J. M.; Shand, W.; Schomaker, V. *J. Am. Chem. Soc.* **1950**, *72*, 4222.
(36) Riveros, J. M.; Wilson, E. B. *J. Chem. Phys.* **1967**, *46*, 4605.
(37) Miyazawa, T. *Bull. Chem. Soc. Jpn.* **1961**, *34*, 691.
(38) Cornibert, J.; Hien, N. V.; Brisse, F.; Marchessault, R. H. *Can. J. Chem.* **1974**, *52*, 3742.
(39) Yan, J. F.; Vanderkooi, G.; Scheraga, H. A. *J. Chem. Phys.* **1968**, *49*, 2713.
(40) Cornibert, J.; Marchessault, R. H. *Macromolecules* **1975**, *8*, 296.
(41) Cornibelt, J.; Marchessault, R. H. *J. Mol. Biol.* **1972**, *71*, 735.
(42) Bunn, C. W.; Turner Jones, A. *Acta Crystallogr.* **1962**, *15*, 105.
(43) Zugenmaier, P.; Sarko, A. *Biopolymers* **1976**, *15*, 2121.
(44) Zugenmaier, P.; Sarko, A. In *Fibre Diffraction Methods*; French, A. D., Gardner, K. H., Eds.; ACS Symposium Series 141; American Chemical Society: Washington, DC, 1980; p 225.
(45) Brisse, F.; Marchessault, R. H.; Perez, S. In *Preparation and Properties of Stereoregular Polymers*; Lenz, R. W., Clardelli, F., Eds.; Reidel: Dordrecht, The Netherlands, 1979; p 407.
(46) Jakeways, R.; Smith, T.; Ward, I. M.; Wilding, M. A. *J. Polym. Sci. Polym. Lett. Ed.* **1976**, *14*, 41.
(47) Cornibert, J.; Marchessault, R. H.; Allegrezza, A. E.; Lenz, R. W. *Macromolecules* **1973**, *6*, 676.
(48) Prud'homme, R. E.; Marchessault, R. H. *Macromolecules* **1974**, *7*, 541.
(49) Prud'homme, R. E.; Marchessault, R. H. *Makromol. Chem.* **1974**, *175*, 2705.
(50) Van Hutten, P. F.; Koning, C. E.; Smook, J.; Pennings, A. J. *Polymer* **1983**, *24*, 237.
(51) Hoogsteen, W.; Pennings, A. J.; ten Brinke, G., submitted for publication in *Colloid Polym. Sci.*
(52) Smook, J.; Pennings, A. J. *Colloid Polym. Sci.* **1984**, *262*, 712.
(53) Hoogsteen, W.; ten Brinke, G.; Pennings, A. J. *Colloid Polym. Sci.* **1988**, *266*, 1003.

Registry No. PLLA (SRU), 26161-42-2; PLLA (homopolymer), 33135-50-1.

Effect of Tricrecyl Phosphate Doping on the Remanent Polarization in Uniaxially Oriented Poly(vinylidene fluoride) Films

Y. Takase,* J. I. Scheinbeim, and B. A. Newman

Department of Mechanics and Materials Science, College of Engineering, Rutgers University, Piscataway, New Jersey 08854. *Received December 13, 1988; Revised Manuscript Received July 17, 1989*

ABSTRACT: Uniaxially stretched films of poly(vinylidene fluoride) were doped (1 wt %) with plasticizer, tricrecyl phosphate (TCP). This slight doping with TCP was found to enhance the amount of remanent polarization in the region of low poling fields (e.g., from 1 to 6 mC/m^2 under E_p = 60 MV/m at 20 °C) and high poling fields (e.g., from 57 to 66 mC/m^2 under E_p = 200 MV/m at 20 °C). The pyroelectric coefficient has shown that the doping enhances a quite stable (up to about 140 °C) remanent polarization after high-field poling (e.g., from 10.2 to 12.5 μC/m^2/K under E_p = 200 MV/m at 20 °C). This is suggestive of a field-induced increase in crystallinity. In addition, the switching of quasi-stable dipoles (those that randomize in the 90–140 °C range) takes place at much lower electric fields than in undoped films. The present data suggest that a small amount of dopant in the noncrystalline regions greatly enhances ferroelectric dipole switching, possibly by acting in the interfacial zone between crystalline and amorphous regions.

Introduction

Plasticized polymers, such as the poly(vinyl chloride)–tricrecyl phosphate (PVC–TCP) system, offer significant advantages in their physical properties such as toughness, flexibility, oil resistance, and nonflammability as well as high electrical resistance when compared to unplasticized polymers.

Recently, it was found in our laboratories that the addition of plasticizer to poly(vinylidene fluoride) (PVF_2) films has a significant influence on their piezoelectric and pyroelectric properties. Sen et al.[1] prepared two different types of samples to examine the effects of TCP doping. One type of sample was unoriented phase II PVF_2 film that was prepared by melt crystallization. The other type of sample was oriented phase I PVF_2 film that was obtained from the phase II film by uniaxial stretching at 54 °C. For doping, the film was immersed in TCP at elevated temperatures.

In the case of the initially unoriented phase II films, the piezoelectric and pyroelectric coefficients of the doped films showed significantly improved values compared to those of the undoped films when poled under identical conditions. The results of X-ray diffraction studies of both types of samples showed that for the doped films, the phase transformation from the nonpolar phase II crystal form to the polar phase I crystal form had taken place at much lower poling fields than for undoped films.

In the case of the uniaxially oriented phase I films, doping also led to a large increase in piezoelectric and pyroelectric response.

Although X-ray diffraction data of the doped films have suggested that some preferential positioning of the dopant at the crystallite boundaries may occur, with no evidence of diffusion of the dopant into the crystalline regions, additional studies are required to gain some understanding of the mechanisms involved.

0024-9297/90/2223-0642$02.50/0 © 1990 American Chemical Society

PVF_2 is a semicrystalline polymer and its crystallinity is usually around 50%[2-5] (recently, perdeuteriated PVF_2 films were found to have much higher crystallinity[6]). Since there was no indication (from X-ray diffraction studies) of the plasticizer diffusing into the crystalline regions,[1] most of the plasticizer must be in solution outside the crystalline regions. The effect of the plasticizer on the bulk properties of the PVF_2 film may therefore be understood in terms of the activity of the dopant on a heterogeneous system that consists of crystalline regions and plasticized amorphous regions and their interface zones.

One possible way to identify the role of plasticizer in this complicated system is to only slightly dope the sample to ensure that the plasticizer does not change too many physical parameters simultaneously (i.e., modulus, dielectric constant, thermal expansion) and to detect any significant effects by some set of sensitive measurements. Our assumption of the minimal effects of the slight doping (about 1 wt % as described later) with plasticizer on the physical properties of the films is based on the fact that a polymer that is ~70 °C above its glass transition temperature (~−50 °C for PVF_2) will exhibit minimal changes in properties at room temperature.

A recent study carried out by Takase et al.[7] on the polarization reversal characteristics of PVF_2 provides suggestions concerning such measurements. They used a γ-ray irradiation technique in order to identify the different roles of dipoles whose arrangement covers a range from an amorphous state to a well-ordered crystalline state. This study was based on the assumption that molecular chains within the crystals are less affected by γ-ray irradiation than chains in the amorphous regions.[8] It was found that the effect of irradiation was most pronounced during the initial stage of the polarization reversal process, i.e., at the nucleation stage.[7] A very likely place for the nucleation process to occur is the interfacial zone between the crystalline and amorphous regions. If we add a small amount of dopant to the PVF_2 film, we should observe an effect that may be a counterpart to the γ-ray irradiation effect, i.e., something that appears not to alter the crystalline regions while slightly altering the amorphous regions and the interface zones.

In the present study, we prepared doped samples by the same immersion method used by Sen et al.[1] but we changed some sample and measurement conditions. We used the same stretched films previously used by several other researchers for polarization reversal measurements,[7,9-12] to examine consistency with previous data. We limited the temperature and time of the immersion process to much less than those used by Sen et al.,[1] so as to minimize change in the physical condition of the crystalline regions, and we then examined the change in remanent polarization, P_r, which is the most fundamental parameter related to piezoelectric and pyroelectric properties.

As a result, we hoped to show some marked effect of the dopant on the electric displacement, D, on the depolarization current (DPC), and on the pyroelectric coefficient, p_y, of the PVF_2 films. On the basis of detailed data obtained under various poling conditions, the role of the dopant in enhancing the remanent polarization was examined.

Experimental Section

Samples used in this study were 7-μm-thick uniaxially oriented PVF_2 films (KF1000) supplied by Kureha Chemical Industry, Co., Ltd. These films are the same as those used in several previous studies[7,9-12] and, in addition, 97% of the crystalline material is in the phase I form.[10] Annealed samples were prepared by heat treatment in vacuum at 120 °C for 2 h. During annealing, the film was mechanically clamped to prevent shrinkage.

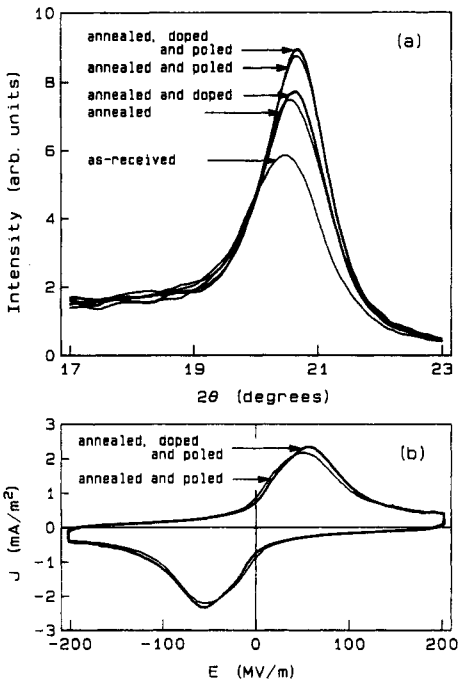

Figure 1. (a) Diffractometer scans (reflection mode) at room temperature of five different samples of uniaxially oriented PVF_2 film: as received, annealed at 120 °C for 2 h, annealed then immersed in TCP at 100 °C for 4 h, annealed then poled under 200 MV/m at 20 °C, and annealed–doped then poled. (b) Current densities versus electric field characteristics during the poling procedure of the last two samples. The period of the triangular shaped electric field was 640 s.

Doped samples were prepared by immersing the annealed films in tricresyl phosphate at 100 °C for 4 h. The temperature and immersion time were much less than those used (130 °C for 24 h) by Sen et al.[1] The dopant content was only about 1% by weight. Hereafter, undoped sample refers to the as-annealed undoped film.

Gold electrodes, each about 3 × 10 mm^2 in area, were deposited on opposing surfaces of the films by vacuum evaporation. All measurements, except X-ray measurements, were carried out by placing the sample in an electrically shielded copper cell that was equipped with a heater and temperature sensor.

X-ray diffraction profiles were obtained at room temperature with a Philips XRG 3100 X-ray generator. Cu Kα radiation filtered with Ni foil was used.

The D–E hysteresis characteristics were measured at 20 °C by using a high-voltage power supply and a picoammeter (Keithley 485) connected in series with the sample. The period of the triangular shaped high-voltage wave was 1000 s.

The pyroelectric coefficient and depolarization current were obtained from samples poled by applying a step voltage pulse of 1-min width at room temperature; then, the thermally stimulated current was measured by the picoammeter as the sample was subjected to heating and cooling cycles at a rate of 2 °C/min.

Operation of various functions in the system were consigned to a microcomputer (IBM-XT), which also performed the task of data processing.

Results

1. X-ray Diffraction Profiles. The diffractometer scans for the five samples, as received, annealed, annealed–doped, annealed–poled, and annealed–doped–poled, in the reflection mode are shown in Figure 1a. Figure 1b shows the current densities, J, obtained during the poling procedure at room temperature for the doped and undoped samples. For the X-ray measurements, all sam-

Table I
2θ Values and Half-Widths, $\beta_{1/2}$, for the (110)(200) Reflection for Uniaxially Oriented Phase I PVF_2 Films

sample	2θ, deg	$\beta_{1/2}$, deg
as received	20.50	1.58
annealed	20.62	1.42
annealed and doped	20.64	1.36
annealed and poled	20.67	1.29
annealed, doped, and poled	20.69	1.26

ples were prepared and chosen so that there were no significant differences in sample dimensions (unmetalized fringe areas and the gold electrodes were removed). Table I shows the 2θ values and half-widths, $\beta_{1/2}$, for the composite (110)(200) reflection of the phase I crystals in the above five samples. It is seen that the annealed sample exhibits a larger 2θ value, a smaller half-width, and a larger peak height than the as-received samples, indicating a decrease in interplanar separation caused by better packing and increased perfection and size of the crystallites. This is the major change found in the diffraction profiles among the five samples.

The doped sample does not exhibit significant change in the 2θ value and the half-width from those of the annealed sample, although there is probably a slight additional annealing effect caused by the immersion in TCP at 100 °C for 4 h. Actually, the annealed sample, which was heat treated by additional annealing at 100 °C for 4 h, also exhibited a similar slight change in 2θ value. The doping process did not cause the phase I crystalline material to transform to other phases. The doping did not broaden the half-width. Therefore, as expected, the low level of dopant did not appear to diffuse into or significantly affect the structure of the crystalline regions.

The poled samples, both doped and undoped, exhibit large secondary changes in their diffraction profiles: a larger 2θ value, a smaller half-width, and a larger peak height than the unpoled samples. This is indicative of a certain amount of crystal growth as well as the better chain packing induced by the electric field. After testing several samples, the doped and poled samples had a tendency to exhibit the largest changes in their X-ray diffraction profiles; a typical result is shown in Figure 1a. The remanent polarization, P_r, obtained by integrating J with respect to time, is 69 and 60 mC/m^2 for the doped and undoped samples, respectively (showing slightly larger values than those obtained in the next section because there was no correction for the dc conduction current). The doped sample exhibits a 15% higher P_r value than the undoped sample. The increase in P_r is consistent with the X-ray diffraction data, indicating a certain amount of crystal growth.

2. *D–E* Hysteresis Characteristics. Parts a and b of Figure 2 show current density, J, and electric displacement, D, respectively, as a function of electric field, E, when the samples are subjected to triangular electric field pulses with maximum fields of 60, 120, and 200 MV/m. The dotted lines represent data for the doped samples and the continuous lines for the undoped samples. In this measurement, the doped sample showed a certain amount of dc conduction. The conduction component consists of an ohmic (linear) component and a nonlinear component. The nonlinear component normally obeys an exponential dependence on the electric field. Figure 2a shows the corrected J versus E characteristics obtained by subtracting the conduction components.

Significant differences are observed between the data of the doped and undoped samples. The doped samples show a well-defined peak on the J–E curves (Figure 2a),

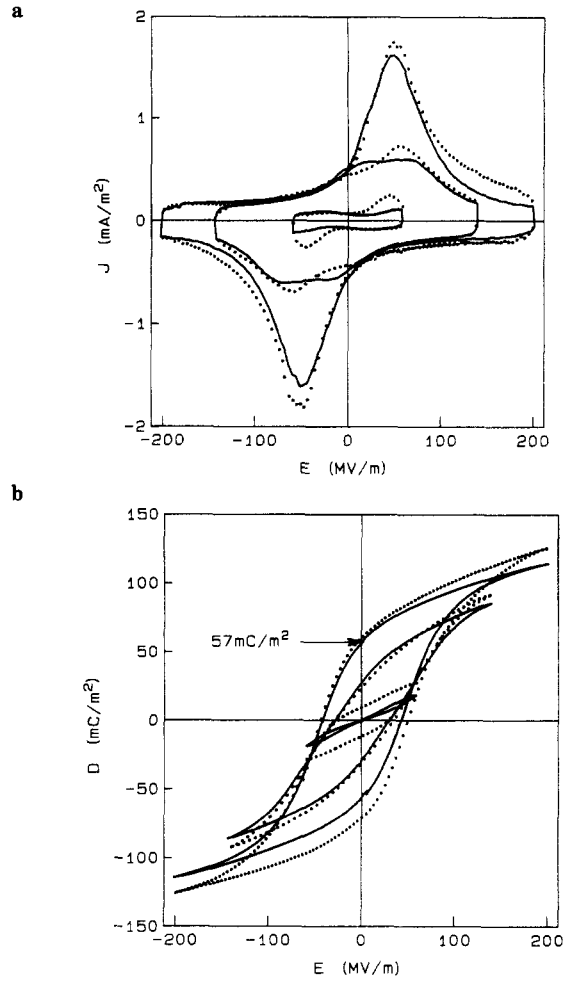

Figure 2. Current densities (a) and electric displacements (b) as a function of electric field when the PVF_2 film is subjected to a triangular electric field with a period of 1000 s at 20 °C. The dotted lines represent data for the doped film and the continuous line for the undoped film.

even if the peak value of E, E_p, is comparatively low, around 60 MV/m. The D–E hysteresis curve (Figure 2b), corresponding to the J–E curve for E_p = 60 MV/m, exhibits a certain amount of remanent polarization (11 mC/m^2). On the other hand, the undoped samples does not show the peak and exhibits a propeller-like D–E hysteresis curve (Figure 2b), which indicates that a small number of dipoles orient under the application of an electric field of 60 MV/m but their orientation is not stable enough to exhibit remanent polarization. These data indicate that ferroelectric dipole orientation is significantly enhanced by the presence of a small amount of TCP outside the crystalline regions of the film.

When the amplitude of the field is 120 MV/m, the doped sample shows a sharp peak on the J–E curve (Figure 2a). Under this field, the undoped sample shows a broad peak on the J–E curve, indicating a polarization reversal originating from some initial field-induced (crystal) dipole orientation. Both samples exhibit almost the same amount of remanent polarization, as is indicated on the D–E hysteresis curves (Figure 2b).

When the field amplitude becomes as high as 200 MV/m, each sample shows a sharp peak on the J–E curve (Figure 2a). The value of remanent polarization of the undoped sample, about 57 mC/m^2 as indicated on the D–E curve (Figure 2b), is known to be almost a saturated value at 20 °C.[11] The doped sample, however, exhibits a value of about 66 mC/m^2 (average value of $+P_r$ and

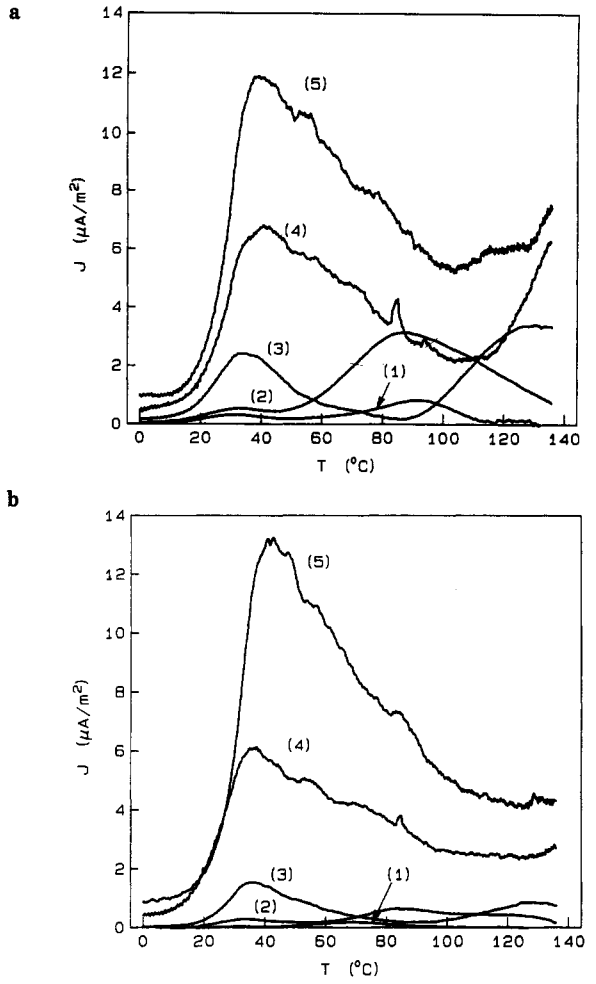

Figure 3. Depolarization current densities for the doped film (a) and the undoped film (b). Curves 1–4 represent the current densities for the films poled by a 1-min step pulse of 20, 60, 120, and 200 MV/m field strength, respectively, and curve 5 represents that for films poled by sequential step pulses of 200 MV/m strength applied in the opposite direction.

$-P_r$ in Figure 2b), which is 16% larger than that of the undoped sample and is consistent with the data in Figure 1b. The J–E curve (Figure 2a) indicates that the increase in P_r of the doped sample is caused by an increase in the current component of polarization reversal in the field region higher than the coercive field. It is surprising that only 1 wt % of dopant enhances the remanent polarization by 16% in the high poling field region as well as greatly enhancing P_r in the low poling field region.

3. Depolarization Current. The D–E hysteresis characteristics show the essential features of ferroelectric polarization reversal and give the value of remanent polarization; however, they do not reveal sufficient information about the polarization reversal mechanism, especially of semicrystalline polymers. In such polymers, not only does the dipole motion differ within the crystallites from that outside but it also differs among crystallites; several physical parameters depend on crystallite size.[13–15] The depolarization current of ferroelectric materials yields information about the thermal stability of the oriented dipoles that reflects their environment in the amorphous regions, the microdomains in small crystallites, and domains in the "usual" crystallites.

The depolarization current densities of the doped and undoped samples are shown in parts a and b of Figure 3, respectively. Curves 1–4 represent the current density for samples poled by a 1-min step pulse of 20, 60, 120,

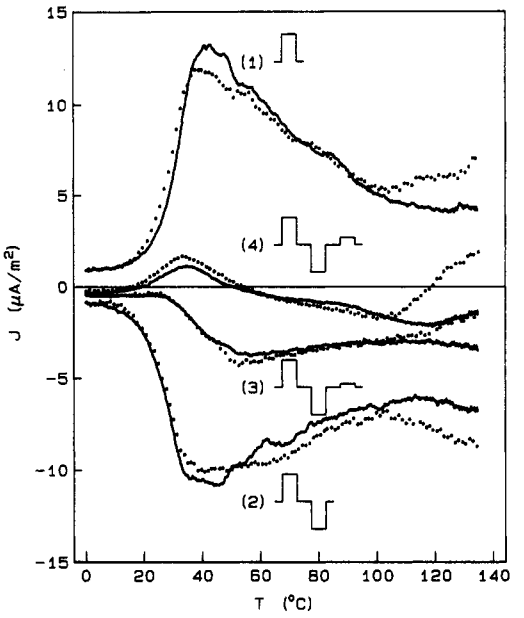

Figure 4. Depolarization current densities showing the polarization reversal process of the doped (dotted lines) and the undoped (continuous lines) films. Curves 1 and 2 represent characteristics of the films poled under +200 and −200 MV/m, respectively. Curves 3 and 4 represent characteristics of the films that are subjected to the poling sequence E_p = +200 MV/m, E_p = −200 MV/m followed by polarization reversal by applying a field of E_p = +20 and +40 MV/m, respectively. Pulses of the poling field are also shown schematically and each step pulse width is 1 min.

and 200 MV/m field strength, respectively, and curve 5 shows that for samples poled by sequential step pulses of 200 MV/m strength applied in the opposite direction. Both samples exhibit one or two current density peaks over the temperature measurement region. A low-temperature peak appears in the temperature region 30–40 °C and the peak shifts slightly to the high-temperature side as the poling field increases. A high-temperature peak appears around 90 °C when the poling field is 20 and 60 MV/m. This peak shifts rapidly to the high-temperature side as the poling field increases.

The marked effect of dopant is also present in the depolarization current. When the poling field is comparatively low, the doped sample shows much higher first and second peaks than those of the undoped sample. The increase in the second peak is prominent after doping; the height is five times larger than that of the undoped sample at E_p = 60 MV/m (see curve 2). When the field is as high as 200 MV/m, the second peak shifts to a temperature region higher than 140 °C and only the broad tail of it can be seen for the doped sample (see curve 4). After applying a second poling field in the reverse direction, the first peak height (of curve 5) increases to twice the size of that (of curve 4) of the sample poled by using a single-step pulse and the height difference of the first peak between the two types of samples is reversed (see curve 5) in Figure 3).

Figure 4 presents the depolarization current versus temperature data, which look at the effects of the polarization reversal process for both the doped (dotted lines) and the undoped (continuous lines) samples. Curve 1 represents characteristics of the sample poled under E_p = +200 MV/m and curve 2 for the sample poled under E_p = +200 MV/m and then E_p = −200 MV/m. These two curves are essentially symmetric with respect to the temperature axis, indicating complete polarization reversal.

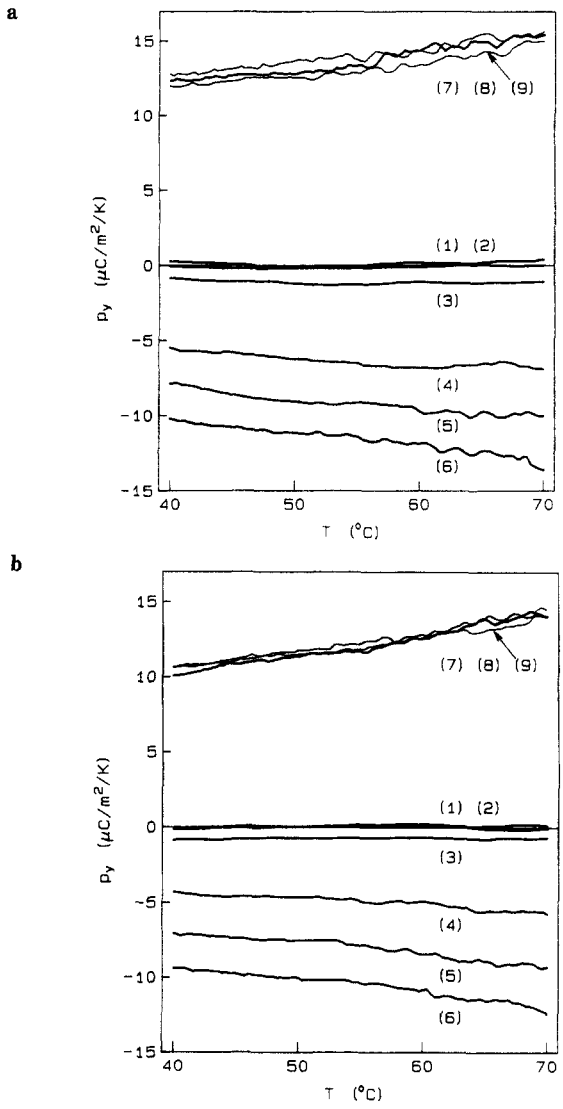

Figure 5. Pyroelectric coefficients in the cooling half-cycle after heating to 140 °C the doped films (a) and the undoped films (b) as a function of temperature. Curves 1–5: poled by a step pulse of 20, 80, 120, 160, and 200 MV/m, respectively. Curve 6: poled by sequential step pulses of +200, −200, and +200 MV/m. Curve 7: poled by a pulse step sequence of +200 MV/m and −200 MV/m. Curve 8: poled by sequential step pulses of +200, −200, and +20 MV/m. Curve 9: poled by sequential step pulses of +200, −200, and +40 MV/m. Each step pulse width is 1 min.

Curves 3 and 4 represent characteristics of the samples that are subjected to the poling sequence +200 MV/m, −200 MV/m, followed by polarization reversal produced by applying a field of E_p = +20 and +40 MV/m, respectively. This was done to gain some further insight into the polarization reversal process. This will be discussed later.

4. Pyroelectric Coefficient. PVF_2 does not show a ferroelectric to paraelectric phase transition before melting occurs; therefore, it is impossible to know the total remanent polarization of the sample by simple integration of the depolarization current (DPC) unless the sample is taken to the melting point. However, we can estimate P_r from the pyroelectric coefficient, p_y, since it is proportional to the remanent polarization.[16]

Parts a and b of Figure 5 show the p_y versus T characteristics of the doped and the undoped samples, respectively. The value of p_y is calculated from the DPC on the cooling cycle after heating up to 140 °C, so that p_y reflects only the high-temperature stable remanent polarization. p_y is obtained from the relation

$$p_{yi} = (J_i - J_{i-1})(t_i - t_{i-1})/(T_i - T_{i-1}) \quad (1)$$

where J is the current density, t is the time, T is the temperature, and the subscript i denotes the sampling number. Curves 1–9 represent data obtained under different poling conditions as follows: (1)–(5), a step pulse of +20, +80, +120, +160, and +200 MV/m, respectively; (6), sequential step pulses of +200, −200, and +200 MV/m; (7), a step pulse of +200 MV/m followed by −200 MV/m; (8), sequential step pulses of +200, −200, and +20 MV/m; and (9), sequential step pulses of +200, −200, and +40 MV/m.

When the poling field is 80 MV/m or lower, the value of p_y is essentially zero, indicating complete decay of the remanent polarization after the process of heating up to 140 °C. Therefore, integration of the depolarization current up to 140 °C gives the remanent polarization; for example, the integration of curve 2 in Figure 3 gives 6 and 1 mC/m^2 under E_p = 60 MV/m for doped and undoped samples, respectively. These values are essentially consistent with the hysteresis data (P_r = 11 and 1 mC/m^2 shown in Figure 2b), since the DPC is measured sometime after poling and some of the unstable polarization has decayed. As the poling field increases up to 120 MV/m, the value of p_y slightly increases for both doped and undoped samples. This is consistent with the DPC data, since the tail of the second peak goes into the temperature region above 140 °C (see Figure 3). The increase in poling field from 120 to 160 MV/m brings about a large increase in p_y, from −0.9 to −5.7 (μC/m^2)/K at 40 °C, for the doped sample and −0.9 to −4.5 (μC/m^2)/K at 40 °C for the as-annealed sample. This is indicative of a large enhancement of the stable remanent polarization, which does not decay by heating up to 140 °C. It is also clear that the stable remanent polarization increases when the sample is poled by a train of electric field step pulses applied in reversed directions. When the sample is poled in a reversed direction, the polarity of p_y reverses. The value of p_y of the doped samples after the reversal is 12.5 (μC/m^2)/K, which is larger by 22% than the 10.2 (μC/m^2)/K of the as-annealed samples. This is also quite consistent with the D–E hysteresis data (16% increase in P_r as shown in Figure 2b).

Discussion

1. Dopant Effect in the Low Poling Field Region. When the samples are poled below about 80 MV/m, the dopant effect is the most prominent. The amount of P_r in the doped sample is several times larger than that of the undoped samples under identical poling conditions. The DPC measurements indicate that P_r originates from the orientation of thermally unstable dipoles, which totally randomize on heating up to 140 °C. The fact that this effect is strongest at low poling fields may indicate that the thermally unstable dipoles are located in an environment that is directly affected by the noncrystalline regions where the dopant exists.

2. Dopant Effect in the High Poling Field Region. A marked dopant effect is observed after polarization reversal: a 15–16% increase in the remanent polarization and a 22% increase in the pyroelectric constant after repeated application of high reversed poling fields. A possible mechanism involved is additional crystal growth at the the interfacial zones, which is indicated by the X-ray diffraction data shown in Figure 1a and is consistent with previous studies.[17] An additional increase in the internal field in the crystalline regions due to an increased in dielectric constant in the amorphous regions and an increase

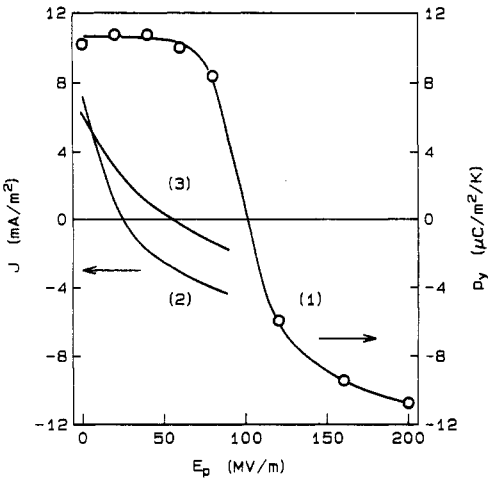

Figure 6. Polarization reversal process reflecting switching of thermally stable and unstable dipoles. Curve 1 is the trace of p_y as a function of a reversed poling field at 40 °C, a part of which is shown in Figure 5b. Curves 2 and 3 are the traces of the depolarization current densities as a function of reversed poling field (in Figure 4) at 135 °C for doped and undoped samples, respectively.

in thermal expansivity may be other mechanisms. In the present experiments, however, the doped samples showed about a 16% increase in P_r, which was almost independent of the dc conduction levels of the samples tested (see Figure 1b and Figure 2b), and the measurements of dielectric constant and mechanical modulus showed no significant measurable change after the doping. The fact that a small amount of dopant produced a large change in the P_r and p_y values suggests to us some catalytic role of the dopant rather than a more macroscopic role related to changes in bulk dielectric constant or mechanical properties.

3. Dopant Effect on the Polarization Reversal Process. In order to further understand the dopant effect, it is useful to examine the two sets of data of DPC versus T (Figure 4) and p_y versus T (Figure 5) since they reveal some details of the process of polarization reversal. Figure 6 shows the behavior of DPC and p_y at a fixed temperature after application of a reversal poling field. Curve 1 is the trace of p_y at 40 °C, a part of which is shown in Figure 5b. Since p_y is obtained in the cooling cycle after heating up to 140 °C, the curve represents the polarization reversal process of the thermally stable dipoles. Curves 2 and 3 are the traces of the depolarization current densities (in Figure 4) at 135 °C for doped and undoped samples, respectively. Since the current is measured in a heating cycle, the curves represent the polarization reversal process of the thermally unstable dipoles. The thermally stable dipoles do not reorient if the antiparallel field is lower than about 80 MV/m and suddenly begin to switch around E_p = 100 MV/m (see curve 1 in Figure 6). This behavior appears to indicate switching of dipoles in the crystalline regions. On the other hand, the thermally unstable dipoles tend to reorient, even if the antiparallel field is lower than 20 MV/m (curves 2 and 3). This behavior suggests that the switching of the thermally unstable or quasi-stable dipoles occurs in the noncrystalline or interface regions. If we define an apparent coercive field, E_c, as the intercept of curves 1, 2, and 3 on the E_p axis, they are about 100, 25, and 55 MV/m, respectively. The large decrease in E_c from 55 to 25 MV/m is one of the most prominent dopant effects in the polarization reversal process. We can see an intimate relation between the decrease in E_c and the data of the hysteresis measurement. The J versus E curves in Figure 2a show that the peak position of the doped sample under E_p = 60 MV/m is about 40 MV/m, while the undoped sample does not show the peak. The peak position of the undoped sample, however, was estimated to be around 90 MV/m from the additional measurement under E_p = 100 MV/m. The peak position under low E_p also represents a coercive field of the quasi-stable dipoles. Therefore, it is considered that more than half of the decrease in coercive field that appeared in both D–E and DPC measurements reflected a prominent doping effect of the quasi-stable dipoles.

It is interesting to note that the behavior of dipoles with different stability in PVF_2 is also clear in the time domain measurement of the polarization reversal.[7] The dopant effect shown by the large decrease in E_c for the unstable dipoles is also quite consistent with the effect of γ-ray irradiation[7] on the polarization switching characteristics. Irradiation suppresses the nucleation probability, while the presence of dopant appears to produce exactly the opposite effect. The dopant effect as well as the γ-ray irradiation effect on the polarization reversal process may provide further information about the nucleation and domain growth process in PVF_2 films.

Conclusions

X-ray diffraction data show that the dopant exists outside the crystalline regions of the film; however, even this small amount of TCP (1 wt %) significantly enhances the low poling field (E_p < 80 MV/m at room temperature) remanent polarization. The polarization originates from thermally unstable dipole orientation, which is suggestive of their environment: interfacial zones between crystalline and amorphous regions. Doping with TCP also enhances the high poling field (E_p > 120 MV/m at room temperature) remanent polarization. The polarization originates from a thermally stable dipole orientation, which is suggestive of a certain amount of crystal growth at the interfacial zones.

In the polarization reversal process, doping with TCP greatly decreases the coercive field of dipoles that might exist at the nucleation sites of polarization domains, i.e., at the interfacial zones. This may provide further information about the nucleation and growth process during polarization reversal in PVF_2 films.

Acknowledgment. This work was supported by DARPA and the Office of Naval Research.

References and Notes

(1) Sen, A.; Scheinbeim, J. I.; Newman, B. A. *J. Appl. Phys.* **1984**, *56*, 2433.
(2) Kakutani, H. *J. Polym. Sci.* **1970**, *8*, 1177.
(3) Murayama, N. *J. Polym. Sci.* **1975**, *13*, 929.
(4) Kepler, R. G.; Anderson, R. A. *J. Appl. Phys.* **1978**, *49*, 1232.
(5) Scheinbeim, J. I.; Chung, K. T.; Pae, K. D.; Newman, B. A. *J. Appl. Phys.* **1979**, *50*, 6101.
(6) Takase, Y.; Tanaka, H.; Wang, T. T.; Caise, T.; Kometani, J. *Macromolecules* **1987**, *20*, 2318.
(7) Takase, Y.; Odajima, A.; Wang, T. T. *J. Appl. Phys.* **1986**, *60*, 2920.
(8) Wang, T. T. *Ferroelectrics* **1982**, *41*, 213.
(9) Furukawa, T.; Date, M.; Fukada, E. *J. Appl. Phys.* **1980**, *51*, 1135.
(10) Takahashi, N.; Odajima, A. *Jpn. J. Appl. Phys.* **1981**, *20*, L59.
(11) Takase, Y.; Odajima, A. *Jpn. J. Appl. Phys.* **1982**, *21*, L707.
(12) Furukawa, T.; Date, M.; Johnson, G. E. *J. Appl. Phys.* **1983**, *54*, 1540.
(13) Kaganov, M. I.; Omel'yanchun, A. N. *Soviet Phys. JETP* **1972**, *34*, 895.
(14) Binder, K.; Hohenberg, P. C. *Phys. Rev.* **1972**, *B6*, 3461.

(15) Odajima, A.; Takase, Y.; Ishibashi, T.; Yuasa, K. *Jpn. J. Appl. Phys. Suppl.* **1985**, *24-2*, 881.
(16) Wada, Y.; Hayakawa, R. *Ferroelectrics* **1981**, *32*, 115.
(17) Takahashi, N.; Odajima, A. *Ferroelectrics* **1981**, *32*, 49.

Dynamics of the β Process in Poly(vinyl chloride)

S. Havriliak, Jr., and T. J. Shortridge*

Modifiers Research Department, Rohm and Haas Co., Bristol, Pennsylvania 19007.
Received February 28, 1989; Revised Manuscript Received March 31, 1989

ABSTRACT: The dielectric relaxation data of Ishida in the β-process region of poly(vinyl chloride) is represented in terms of the relaxation function proposed by Havriliak and Negami using the multiresponse techniques developed by Havriliak and Watts to evaluate the parameters and their dependence on temperature. These parameters are compared with those reported by the authors on the viscoelastic β process in poly(vinyl chloride). The three dynamic parameters and their dependence on temperature for the two processes are similar though not all of them are within their 95% confidence limits. The dynamics of the dielectric and viscoelastic β process in poly(vinyl chloride) and polycarbonate are compared. The mechanism for the β process is discussed in terms of the polymer segment orientation model (segment flips) proposed by the authors earlier, with the general model of Mansfield and the ring flip model for polycarbonate by Perchak et al.

Introduction

This paper is another in a series of papers directed at a better understanding of chain dynamics in the glass phase of polymers. Some of these papers reported on the viscoelastic β process in poly(vinyl chloride) (PVC)[1,2] or in polycarbonate (PC).[3] Another[4] reported on the tensile yield properties of PVC as a function of molecular weight, strain rate, and temperature using an approach first proposed by Eyring and co-workers,[5] then extended by Roetling to some polyacrylics[6,7] and to poly(propylene),[8] and also applied to PVC by Bauwens-Crowet et al.[9] In another paper a comparison between the viscoelastic and published dielectric relaxation data of Smith et al.[10] for PC was reported.[11] The approach taken in these papers is based on the following: First the dielectric and viscoelastic β processes are represented in terms of an expression first proposed to represent dielectric α and β relaxation processes. Then tensile yield studies are represented in terms of Roetling's modification of Eyring's model. Finally, the activation energies from the various processes are compared.

There are two important reasons for such an study. First, thermodynamic theories[12] of the glass transition temperature such as those based on the pioneering work of Gibbs et al.[13] seem to suggest that the glass phase is a motionless state, similar to crystals in which polymer chains are "frozen-in place" so that all long-range motions are prohibited. The β process in polymers, usually measured at low strains, ca. 0.1%, and in the glass phase is often considered to be an oscillation about some mean or fixed equilibrium position. This view cannot not represent the mechanism for the large deformations encountered during tensile yielding. This immobilized view of the glass phase is in contradiction to the (limited) correlation observed between the tensile yield studies and viscoelastic as well as dielectric results cited above. Mansfield[14] proposed a jumping model for dielectric α and β dispersions in polymers that is remarkably similar to Eyring's[5] for tensile yielding or Bueche's model[15] for segmental jumping. Such studies may provide a penetrating view of the polymer chain dynamics that occurs in the glass phase.

While the first reason is fundamental to the understanding of the polymeric glass phase, the second reason for such comparative studies is for practical reasons. Many ASTM-type impact tests that characterize the toughness of polymers do not give results that are interpretable to the polymer scientist in terms of polymer structure or chain dynamics. A simple analysis[16,2] of these tests suggest that they essentially measure the energy to break while the specimen is loaded in tension at not only high strain rates but also strain rates that depend on test methods. In addition test specimen preparation, i.e. milling, bottle blowing, is an important aspect of this test. In other words the connection between ASTM impact tests and polymer chain dynamics of the glass phase may be the pioneering work of Eyring and his rate theory that is based on Maxwell–Boltzmann statistics.

The objective of this work is to analyze the dielectric relaxation data for the β process of PVC reported by Ishida[17] and compare them to the viscoelastic results reported by the writers in terms of the concepts mentioned above. In addition the dynamics of the β processes in PVC and PC will be compared.

Estimation of the Parameters

Dielectric Data. A complex plane plot for PVC taken from the work of Ishida[17] covering the temperature range that defines the β process and used in the analysis is given in Figure 1.

Numerical Data. Havriliak and Negami[18] proposed eq 1 to represent the complex dielectric constant, $\epsilon^*(\omega)$, as a function of radian frequency $\omega = 2\pi f$ where f is in hertz, at constant temperature. In this expression, $\epsilon^*(\omega) = \epsilon'(\omega) + i\epsilon''(\omega)$ is the complex dielectric constant and $\epsilon'(\omega)$ is the real or storage part of the complex dielectric constant while $\epsilon''(\omega)$ is the imaginary

$$\frac{\epsilon^*(\omega) - \epsilon_\infty}{\epsilon_0 - \epsilon_\infty} = \{1 + (i\omega\tau_0)^\alpha\}^{-\beta} \quad (1)$$

0024-9297/90/2223-0648$02.50/0 © 1990 American Chemical Society